Supporting Information

Theoretical and Experimental Studies: Cu(I)/Cu(II) Catalytic Cycle in CuI/Oxalamide-Promoted C-N Bond Formation

Devita V. Morarji and Kamlesh K. Gurjar*

Chemical Department, VGEC, Ahmedabad, Gujarat, India 382424

gurjarkamlesh@vgecg.ac.in

Contents

Estimation of Activation Barriers for Single Electron Transfer by Marcus Theory

1. **Marcus-Hush Model for the Outer Sphere Electron Transfer (ET)**[1–4]

The total reorganization energy is given by:

$$\lambda = \lambda_0 + \lambda_i$$

Where λ_i is the inner reorganization energy for the reactants and λ_0 the solvent reorganization energy. λ_i instepwise electron transfer reactions is usually small so we neglect it, therefore, $\lambda = \lambda_0$ and λ_0 can be calculated from:

$$\lambda_0 = (332\text{kcal/mol})\left(\frac{1}{2a_1} + \frac{1}{2a_2} - \frac{1}{R}\right)\left(\frac{1}{\varepsilon_{op}} - \frac{1}{\varepsilon}\right)$$

Where a_1 and a_2 are the radii of the molecules involved in ET ($CCS3\ d = 12.4$; $a_1 = 6.2$; $PhCl\ d = 5.9$; $a_2 = 3$), $R = a_1 + a_2 (= 9.2)$, ε_{op} is the optical dielectric constant (for DMSO $= 2.18$) and ε is the static dielectric constant (for DMSO $= 47.2$)

As a result, we get: $\lambda = \lambda_0 = 20.13534\ kcal/mol$

According to the Marcus theory,

$$\Delta G_{ET'}^{\ddagger} = \Delta G_0^{\ddagger}\left(1 + \frac{\Delta G_r}{4\Delta G_0^{\ddagger}}\right)^2$$

Where ΔG_r is the reaction energy ($= 30.1\ kcal/mol$), and $\Delta G_0^{\ddagger}$ is the intrinsic barrier for the outer-sphere electron transfer. $\Delta G_0^{\ddagger}$ is related to λ by: $\Delta G_0^{\ddagger} = \frac{\lambda}{4} (= 5\ kcal/mol)$.

As a result: $\Delta G_{ET'}^{\ddagger} = 31.4\ kcal/mol$. Therefore:

$$\Delta G_{ET}^{\ddagger} = \Delta G_{ET'}^{\ddagger} + 9.6 = 41\ kcal/mol$$

2. **Savéant's Model for the Concerted/Inner Sphere Electron Transfer (ET)**[5–7]

$$\Delta G_0^{\ddagger} = \frac{\lambda}{4} = \frac{\lambda_0 + \lambda_i + BDFE}{4}$$

Where $BDFE = 81.5$ (DFT calculated).[8]

Resulting in $\Delta G_0^{\ddagger} = 25.4$

Using this value in the Marcus equation, we get:

$$\Delta G_{ET'}^{\ddagger} = 42.7$$

$$\Delta G_{ET}^{\ddagger} = \Delta G_{ET'}^{\ddagger} + 9.6 = 52.3\ kcal/mol$$

Table S1. Effect of Dispersion Correction (DFT-D3) on the Overall Energy Barrier

| Mechanism	Without dispersion correction	With dispersion correction (DFT-D3)
OA	85.33808646	74.40562466
HAT	78.78500997	76.16264986
SET	39.71755465	39.56946252
σ-bond metathesis	97.99683	------
π-complexation	103.677	------

No significant effect has been noticed in HAT and SET mechanisms. In OA, the energy is slightly overestimated in calculations without dispersion correction. However, OA is not the favorable reaction path; therefore, the results do not get affected.

Table S2. Overall Energy Barrier for SET Mechanism Considering CCS1 and CCS2

CCS	Energy barrier for SET (without dispersion correction)
CCS1	98.2 kcal/mol
CCS2	99.4 kcal/mol

Experimental Section

**Experimental set-up for In situ UV-vis spetrocopic study:**
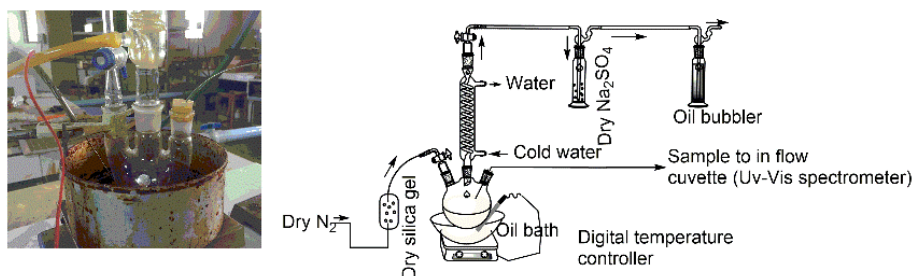
Material availability and Instruments:

IR spectra were recorded on FTIR - Bruker Alpha ATR (ZnSe).
NMR: JEO Resonance 400MHz.
We obtained AR Grade Oxalyl chloride from Avra Chemicals, India; and the other chemicals from Finar Chemicals, Ahmedabad, India. They were used without any further purification.

Synthesis of ligand L1 (N,N`-diphenylethanediamide):
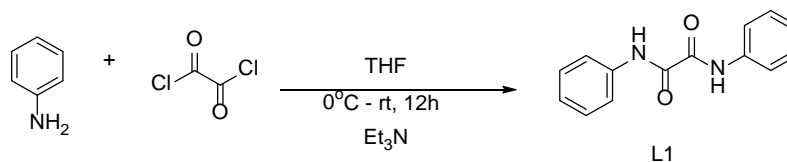
Known compound L1 was synthesized by a previously reported method.[9,10] 0.317 g (1 equiv) of oxalyl chloride was mixed in 5 mL dry THF in a beaker (solution 1). In a round bottom flask, 0.5 g (2.4 equiv) of aniline and Et$_3$N (1 mL) solution was prepared in 5 mL THF (solution 2). Both solutions were under ice bath. Solution 1 was added drop by drop to the solution 2. A white precipitate was instantly formed and the solution was continuously stirred overnight at room temperature. On the next day, the crude was filtered and washed with water and cold diethyl ether to remove the unreacted aniline. The isolated product (L1) was dried in vacuum at 50°C for 4 h, and a fine white powder was obtained, which was used without further purification. The compound was analyzed by NMR, FTIR and Mass spectroscopy.[11,12]

^{1}H NMR (400 MHz, DMSO-d_6) δ 10.81 (s, 2H), 7.84-7.12 (m, 10H), ^{13}C NMR (100.5 MHz, DMSO-d_6) δ 159.1, 138.17, 132.6, 128.38, 125.16,FTIR (ATR-ZnSe, Bruker-alpha) WN (cm^{-1}) 3301.71, 1666, 1594.86, 1496.63, 1266, 1157.37, 754.16, 684.62.
EI-MS m/z 51, 65, 77, 93 (base peak), 120, 240 (parent peak). Calculated Exact Mass: 240.09 (C$_{14}$H$_{12}$N$_2$O$_2$).
The melting point (methanol) was noted, 254-255°C (Lit.255 °C)[10]

Other intermediates were not synthesized and not isolated (except L1). They have been observed in the solution.

In Situ UV-vis spectrum: In a double neck round bottom flask with a magnetic stirrer and under continuous N$_2$ gas purging, a solution of 0.2 mL aniline, 0.5 mL PhCl (2 equiv), L1 0.12 g (20%) and 20 mL DMSO, was prepared. Sequentially, dried K$_3$PO$_4$ (2 equiv) and CuI 0.05 g (10%) were added. The mixture was refluxed at 120 °C for approximately 3 h. The spectrum was recorded by passing the reaction mixture into an in-flow quartz cuvette (10 mm path length) under nitrogen. The same reaction was left overnight at 120 °C. Initially, the mixture had a light brown color and with time it became much darker. The mixture was filtered to remove the solvent, and the final crude had a light yellowish color.

FTIR spectrum: The FTIR analysis of the same crude mentioned above was recorded. The spectrum indicates the conversion of aniline (aniline – NH$_2$ bands disappear) and a single N-H band of diphenylamine appears (3395 cm^{-1}, N-H). N-H band of Ligand L1 appears at 3301 cm^{-1}.
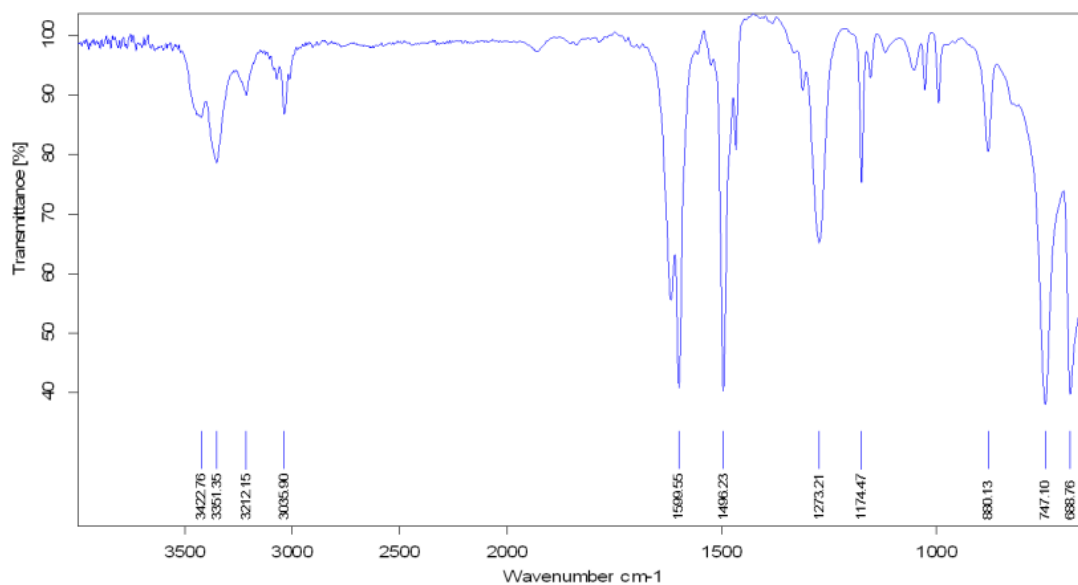
FTIR Analysis
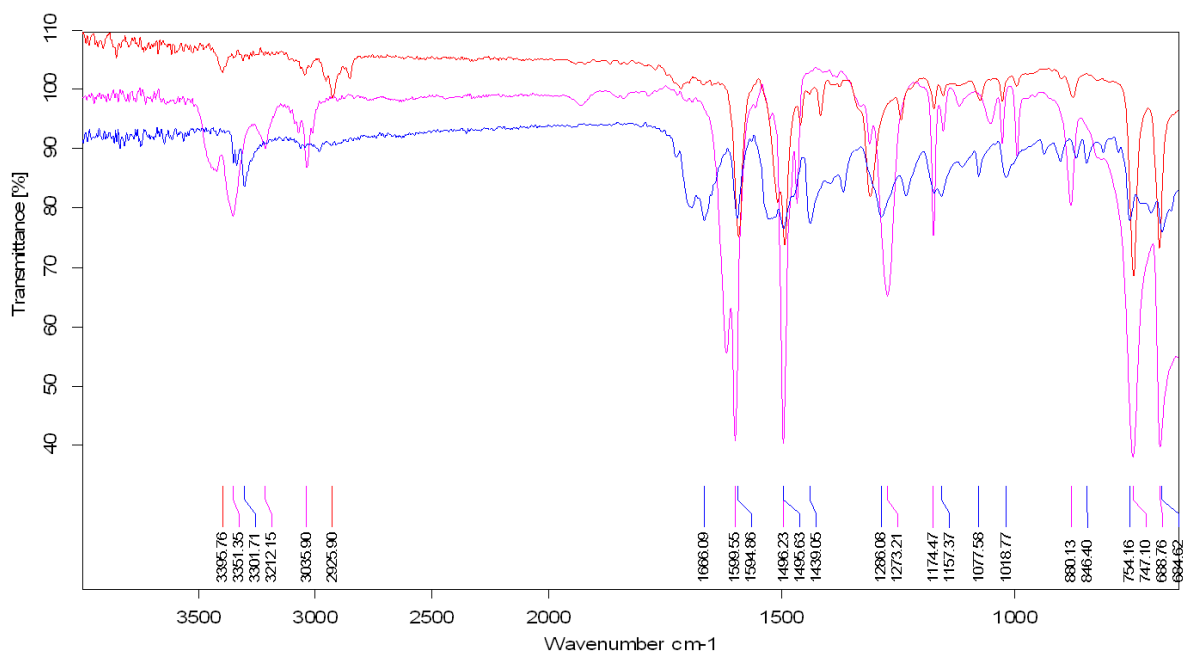
C:\D\C-N\L1.0	L1	Instrument type and / or accessory	03/08/2018
C:\D\C-N\COLUMN CRUDE.0	COLUMN CRUDE	Instrument type and / or accessory	19/12/2018
C:\FTIR_OTHER\ANILINE.0	ANILINE	Instrument type and / or accessory	28/02/2017

Page 1/1

Figure S1. FTIR spectra of L1 (blue), aniline (pink), and crude product of reaction (red).

| C:\FTIR_OTHER\ANILINE.0 | ANILINE | Instrument type and / or accessory | 28/02/2017 |

Page 1/1

Figure S2. FTIR spectrum of aniline

S5
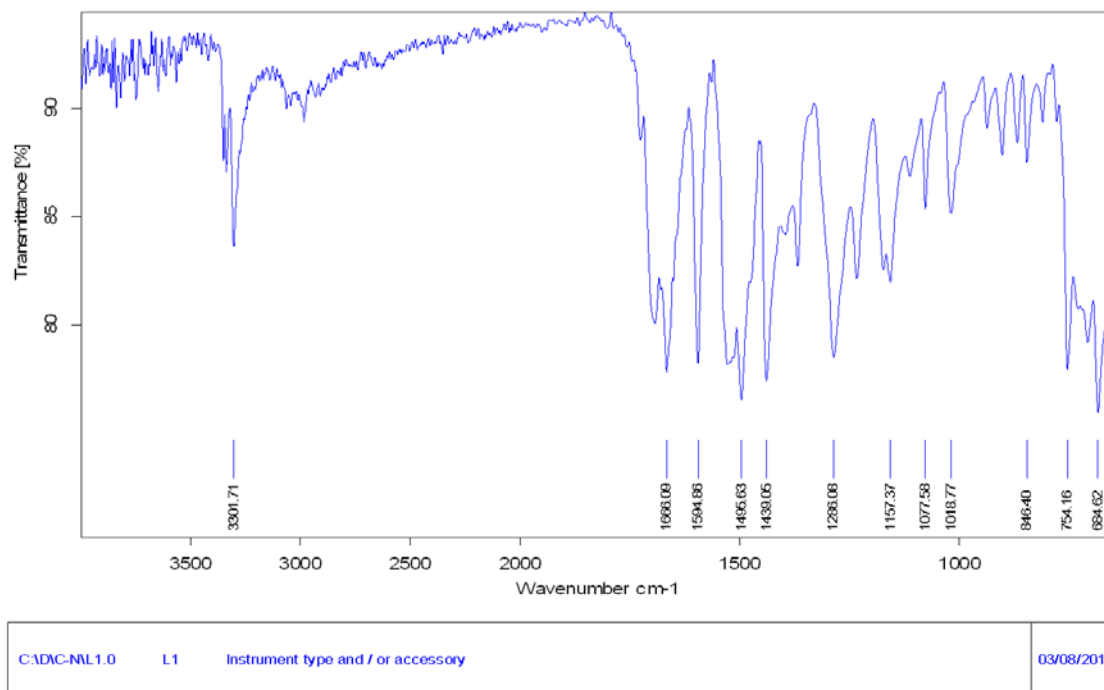
Figure S3. FTIR spectrum of L1

Figure S4. Simulated IR spectrum of L1

GC-MS Analysis

Figure S5. Chromatogram of the crude product from in situ UV-vis spectroscopic studies.

Figure S6. Mass spectrum of diphenylamine **a.** sample and **b.** NIST library search.

<< Target >>
Line#:30 R.Time:52.492(Scan#:5700) MassPeaks:487
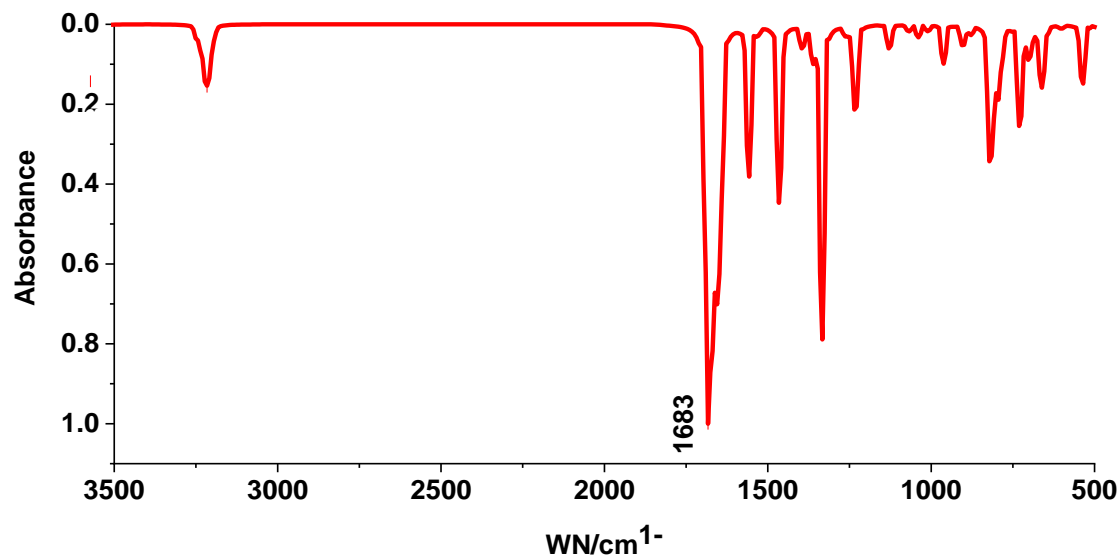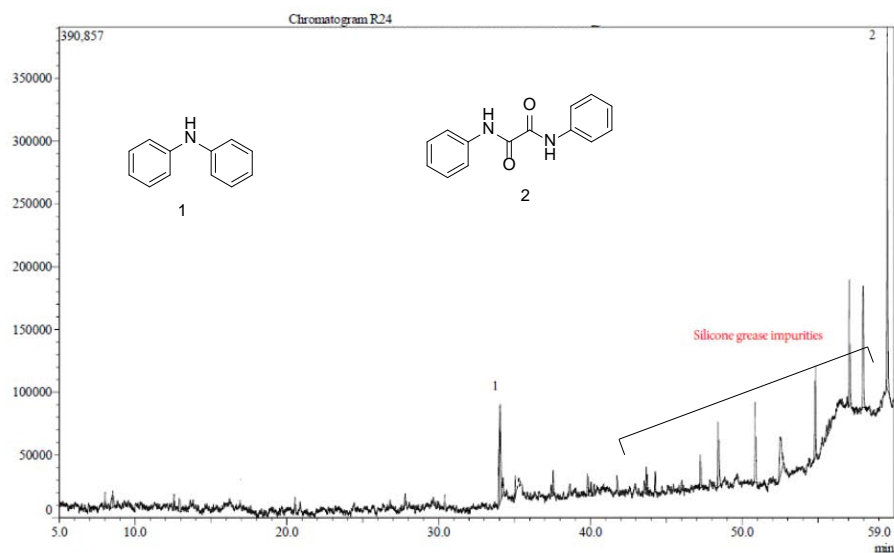RawMode:Averaged 52.483-52.500(5699-5701) BasePeak:93.05(5963)
BG Mode:Calc. from Peak Group 1 - Event 1
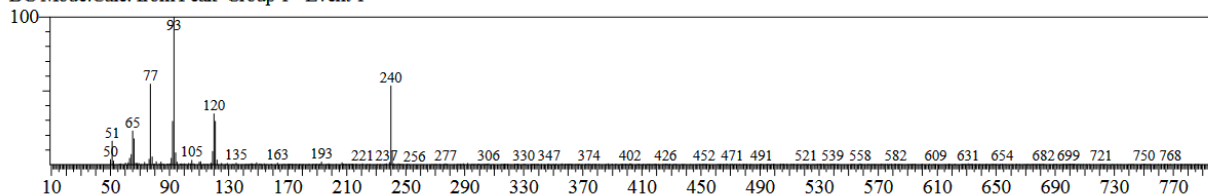
Hit#:1 Entry:72066 Library:NIST11.lib
SI:94 Formula:C14H12N2O2 CAS:620-81-5 MolWeight:240 RetIndex:2366
CompName:Ethanediamide, N,N'-diphenyl- $$ Oxanilide $$ N,N'-Diphenyloxamide $$ Oxalanilide $$ Oxamide, N,N'-diphenyl- $$ Oxanilid $$ Oxaldianilid
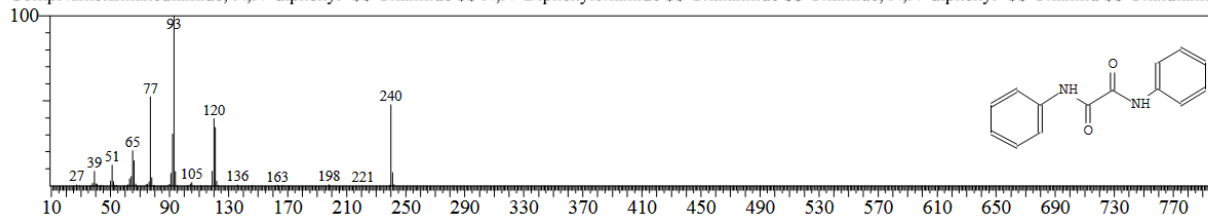
Figure S7. Mass spectrum of N,N'-diphenyl oxamide, **a.** sample and **b.** NIST library search.
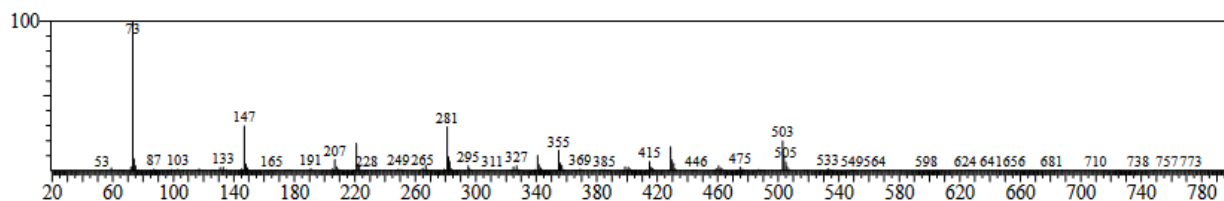
Hit#:1 Entry:209586 Library:NIST11.lib
SI:79 Formula:C16H50O7Si8 CAS:19095-24-0 MolWeight:578 RetIndex:1710
CompName:Octasiloxane, 1,1,3,3,5,5,7,7,9,9,11,11,13,13,15,15-hexadecamethyl- $$ 1,1,3,3,5,5,7,7,9,9,11,11,13,13,15,15-Hexadecamethyloctasiloxane # $
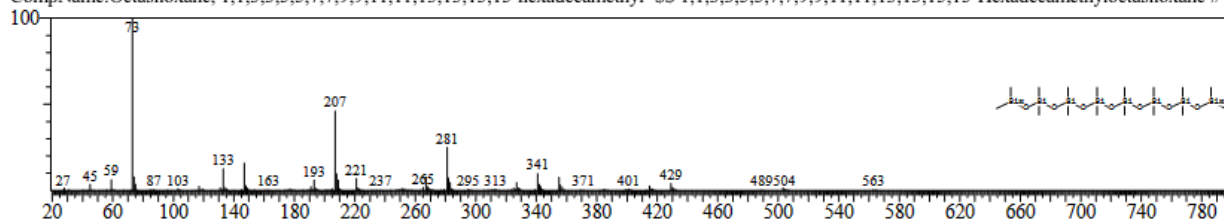
Figure S8. Mass spectrum of silica, **a.** impurities and **b.** NIST library search.

NMR Analysis
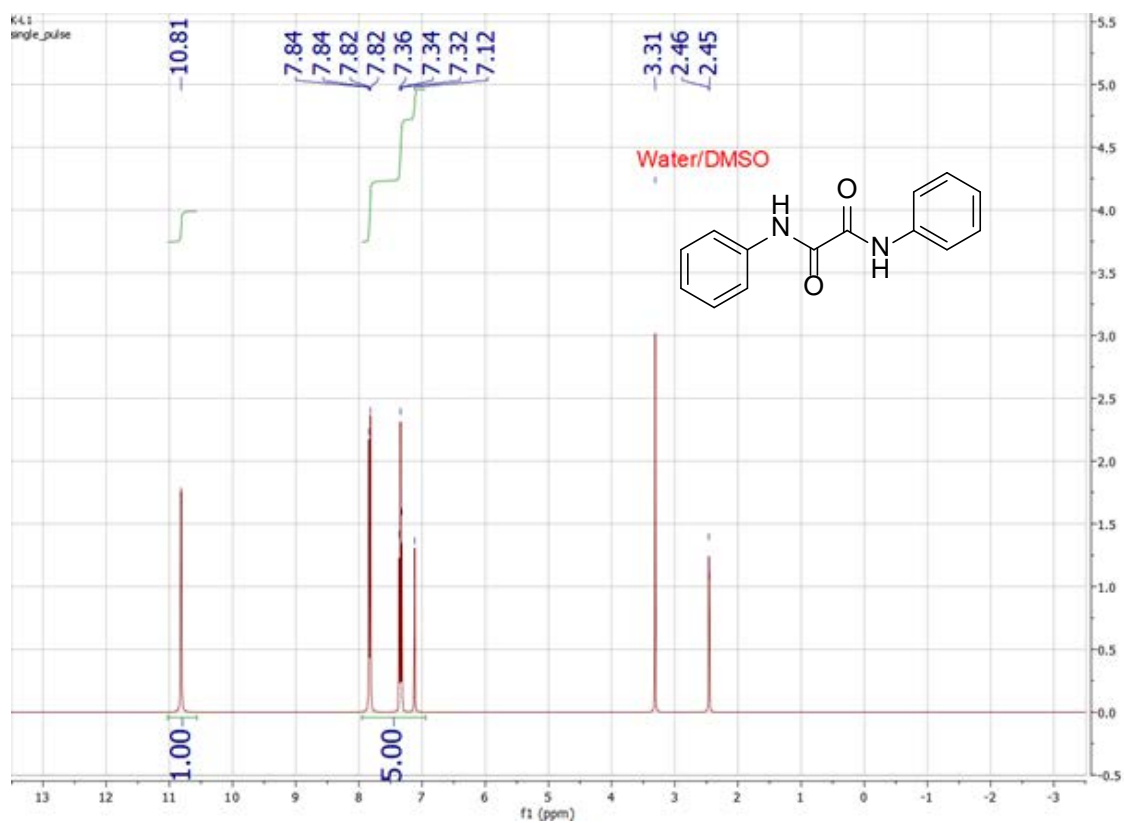
Figure S9. NMR analysis of L1 in DMSO-d_6.
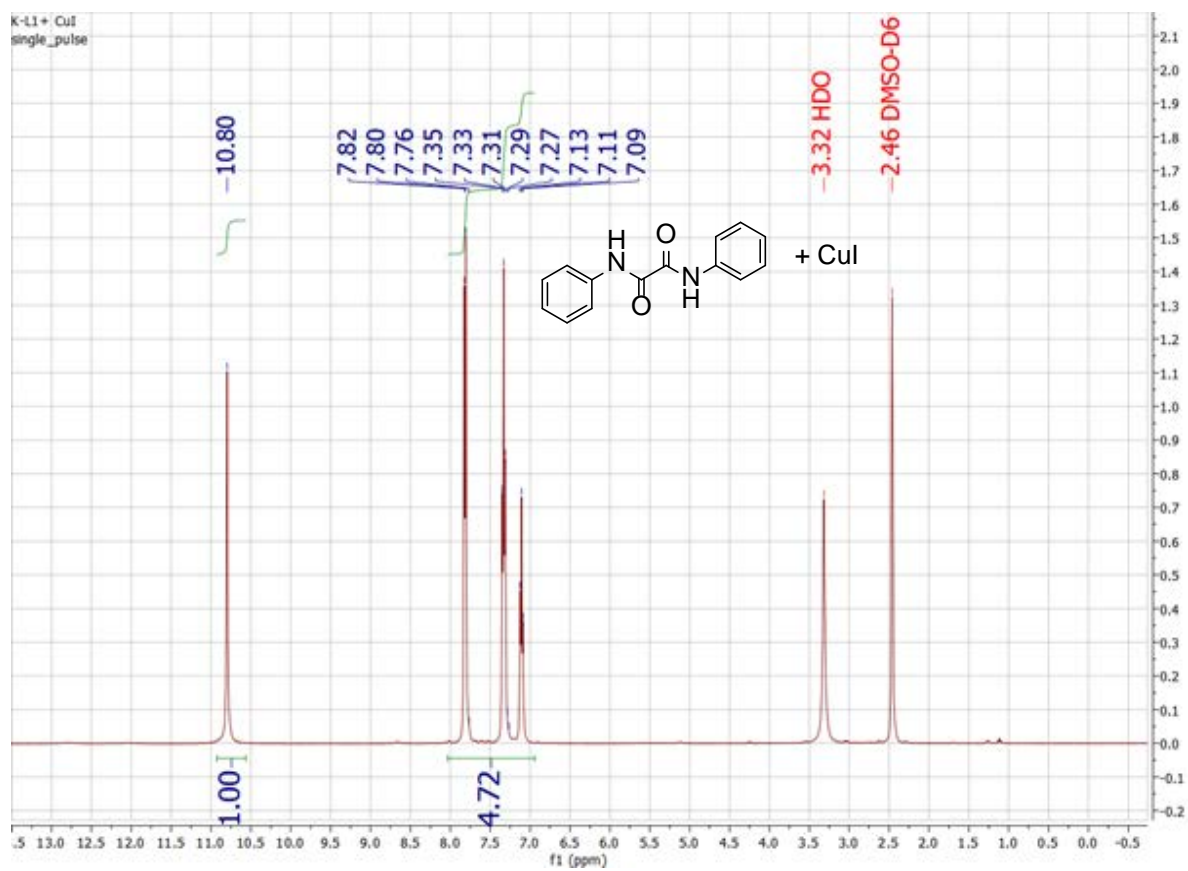
Figure S10. NMR analysis of the solution of L1 and CuI in DMSO-d_6.
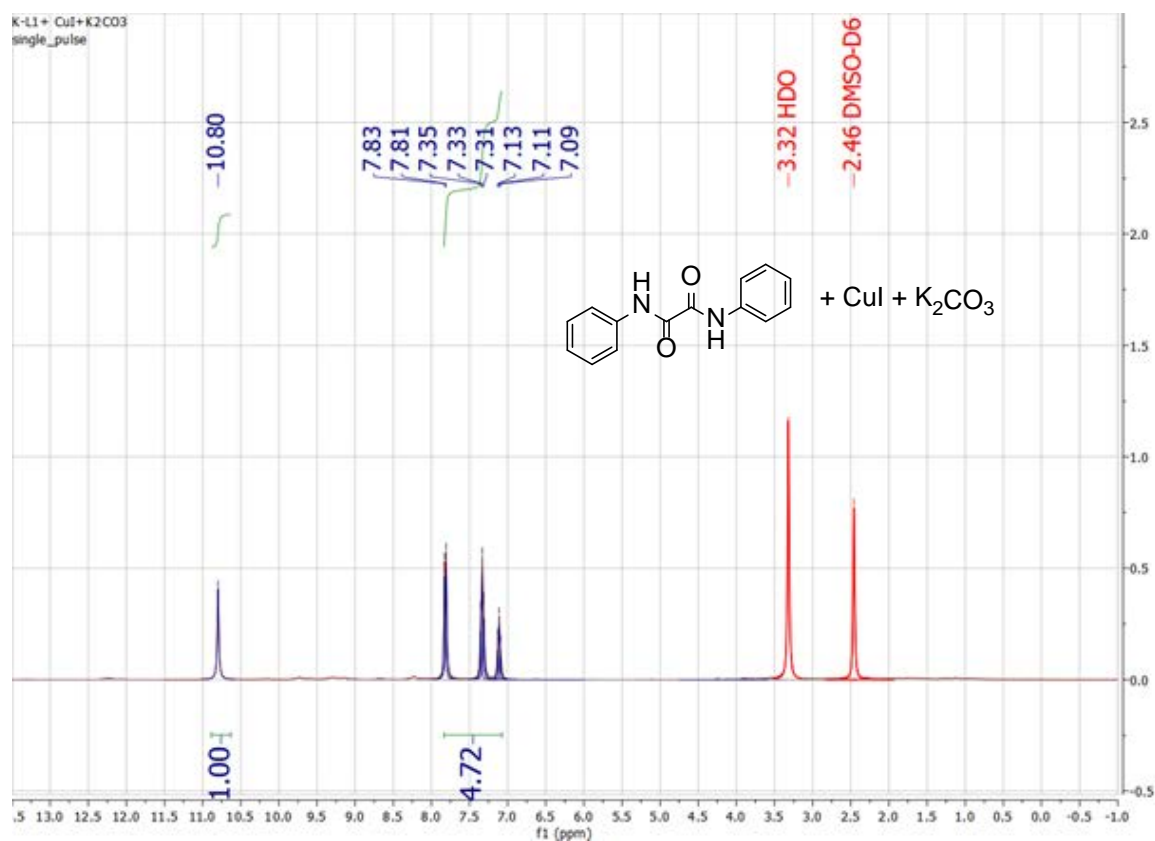
Figure S11. NMR analysis of the solution of L1, CuI, and K$_2$CO$_3$ in DMSO-d_6.
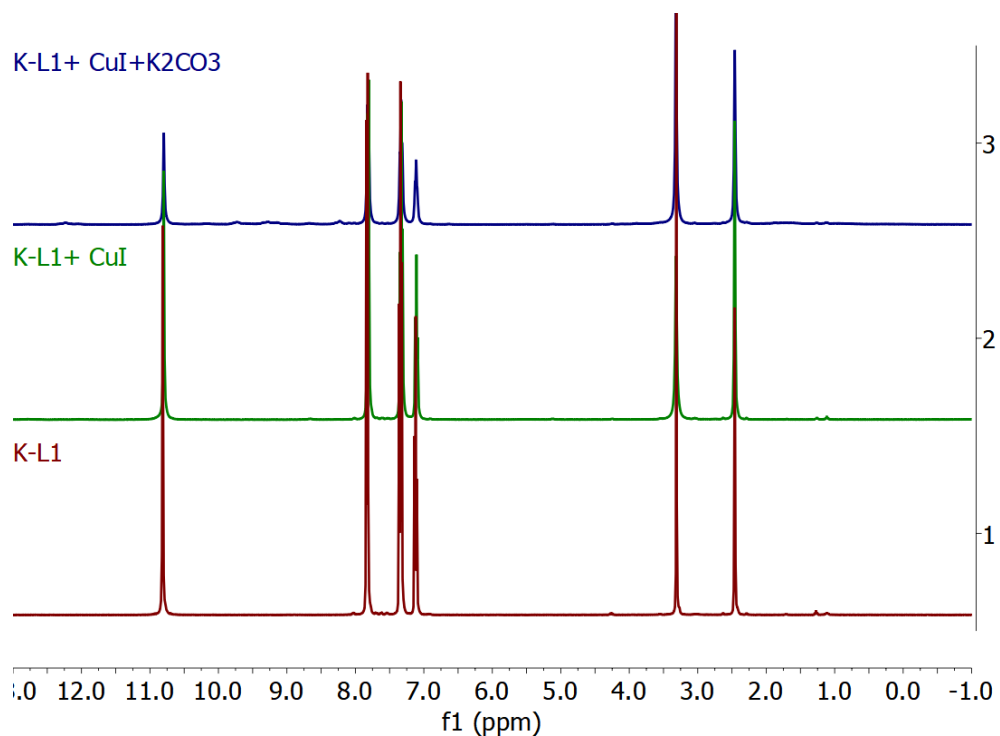
Figure S12. Stacked NMR spectra of L1, L1 + CuI and L1 + CuI + K₂CO₃, in DMSO-*d₆*; Chemical shift δ in -NH and phenyl-H.

CV Analysis

The cyclic voltammetry was performed at CHI660E electrochemical workstation, in a three-electrode cell under continuous N_2 purging at room temperature, at a scan rate of 0.04 Vs^{-1}.The working electrode was a glassy carbon disk (area = 0.071 cm^2), and the counter- and reference-electrodes were platinum wires. Ten scans were taken for each sample for a 10 mL solution of degassed and dried DMSO containing, sequentially, L1 (40 mM); K_3PO_4 (base) (40 mM); CuI (10 mM); Aniline (40 mM); and PhCl (40 mM).
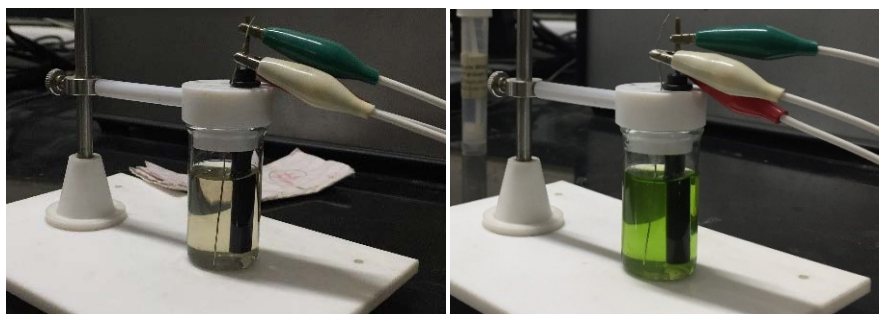
Figure S13. Initial and final colors of the solution noticed during the CV analysis.

S12
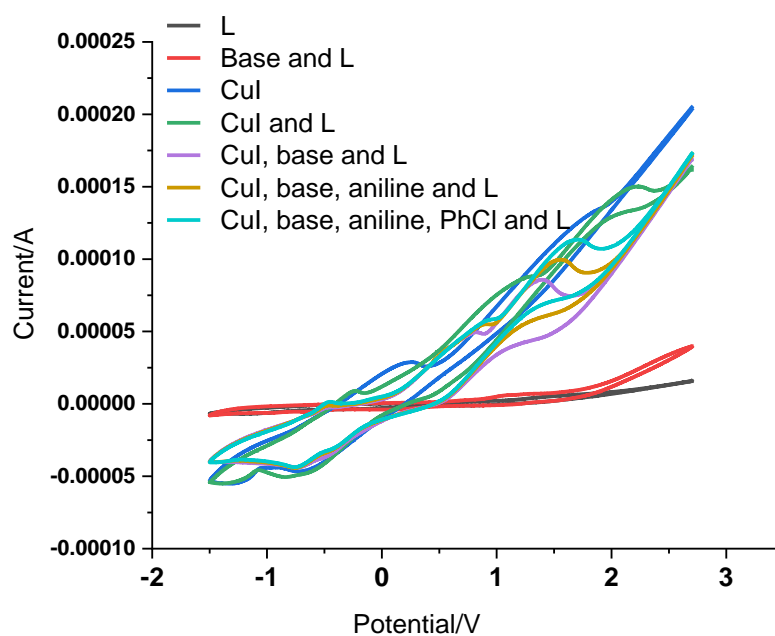
Figure S14. Cyclic voltammograms

L2

-0.0288 eV ——— LUMO

-0.15229 eV ——— HOMO
CCS3

2.85 kcal/mol
0.12349 eV
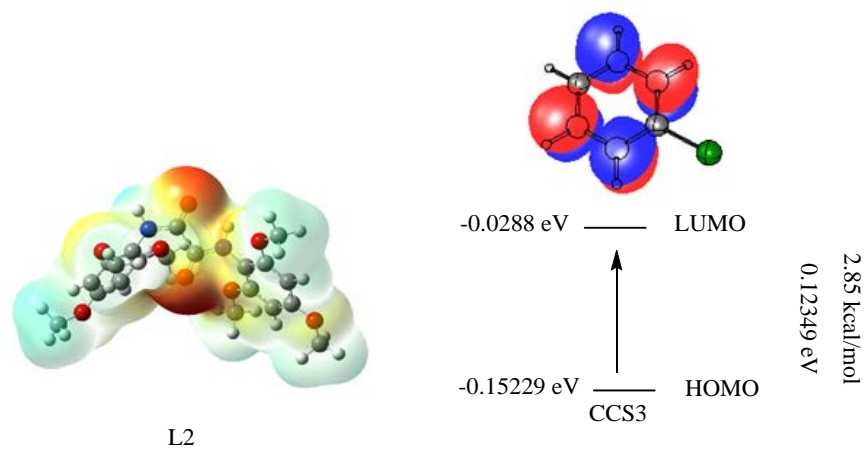
Figure S15. Electrostatic potential map and electron density of L2. FMO analysis of CCS3 and PhCl.

References

(1)   Marcus, R. A. On the Theory of Oxidation-Reduction Reactions Involving Electron Transfer. *J. Chem. Phys.* **1956**, *24* (5), 966–978.

(2)   Marcus, R. A. On the Theory of Oxidation-Reduction Reactions Involving Electron Transfer. III. Applications to Data on the Rates of Organic Redox Reactions. *J. Chem. Phys.* **1957**, *26* (4), 872–877.

(3)   Hush, N. S. Adiabatic Rate Processes at Electrodes. I. Energy-Charge Relationships. *J. Chem. Phys.* **1958**, *28* (5), 962–972.

(4)   Marcus, R. A.; Sutin, N. Electron Transfers in Chemistry and Biology. *Biochim. Biophys. Acta, Rev. Bioenerg.* **1985**, *811* (3), 265–322.

(5)   Saveant, J. M. A Simple Model for the Kinetics of Dissociative Electron Transfer in Polar Solvents. Application to the Homogeneous and Heterogeneous Reduction of Alkyl Halides. *J. Am. Chem. Soc.* **1987**, *109* (22), 6788–6795.

(6)   Saveant, J. M. Dissociative Electron Transfer. New Tests of the Theory in the Electrochemical and Homogeneous Reduction of Alkyl Halides. *J. Am. Chem. Soc.* **1992**, *114* (26), 10595–10602.

(7)   Saveant, J. M. Electron Transfer, Bond Breaking, and Bond Formation. *Acc. Chem. Res.* **1993**, *26* (9), 455–461.

(8)   Ahmad, K.; Khan, B. A.; Akram, B.; Khan, J.; Mahmood, R.; Roy, S. K. Theoretical Investigations on Copper Catalyzed {CN} Cross-Coupling Reaction between Aryl Chlorides and Amines. *Comput. Theor. Chem.* **2018**, *1134*, 1–7.

(9)   Zhou, W.; Fan, M.; Yin, J.; Jiang, Y.; Ma, D. CuI/Oxalic Diamide Catalyzed Coupling Reaction of (Hetero)Aryl Chlorides and Amines *J. Chem. Phys.* **2015**, *137* (37), 11942–11945.

(10) Santana, M. D.; García, G.; Julve, M.; Lloret, F.; Pérez, J.; Liu, M.; Sanz, F.; Cano, J.; López, G. Oxamidate-Bridged Dinuclear Five-Coordinate Nickel(II) Complexes: A Magneto−Structural Study. *Inorg. Chem.* **2004**, *43* (6), 2132–2140.

(11) Shainyan, B. A.; Ustinov, M. V.; Bel'skii, V. K.; Nindakova, L. O. Diamines Having a C2 Symmetry. Synthesis and Application as Ligands in the Hydrogenation of Prochiral Substrates over Rhodium Complexes. *Russ. J. Org. Chem.* **2002**, *38* (1), 104–110.

(12) Parkinson, E. I.; Hatfield, M. J.; Tsurkan, L.; Hyatt, J. L.; Edwards, C. C.; Hicks, L. D.; Yan, B.; Potter, P. M. Requirements for Mammalian Carboxylesterase Inhibition by Substituted Ethane-1,2-Diones. *Bioorg. Med. Chem.* **2011**, *19* (15), 4635–4643.

Computational full citation:

M. J. Frisch, G. W. Trucks, H. B. Schlegel, G. E. Scuseria,
M. A. Robb, J. R. Cheeseman, G. Scalmani, V. Barone, B. Mennucci,
G. A. Petersson, H. Nakatsuji, M. Caricato, X. Li, H. P. Hratchian,
A. F. Izmaylov, J. Bloino, G. Zheng, J. L. Sonnenberg, M. Hada,
M. Ehara, K. Toyota, R. Fukuda, J. Hasegawa, M. Ishida, T. Nakajima,
Y. Honda, O. Kitao, H. Nakai, T. Vreven, J. A. Montgomery, Jr.,
J. E. Peralta, F. Ogliaro, M. Bearpark, J. J. Heyd, E. Brothers,
K. N. Kudin, V. N. Staroverov, T. Keith, R. Kobayashi, J. Normand,
K. Raghavachari, A. Rendell, J. C. Burant, S. S. Iyengar, J. Tomasi,
M. Cossi, N. Rega, J. M. Millam, M. Klene, J. E. Knox, J. B. Cross,
V. Bakken, C. Adamo, J. Jaramillo, R. Gomperts, R. E. Stratmann,
O. Yazyev, A. J. Austin, R. Cammi, C. Pomelli, J. W. Ochterski,
R. L. Martin, K. Morokuma, V. G. Zakrzewski, G. A. Voth,
P. Salvador, J. J. Dannenberg, S. Dapprich, A. D. Daniels,
O. Farkas, J. B. Foresman, J. V. Ortiz, J. Cioslowski,
and D. J. Fox, Gaussian, Inc., Wallingford CT, 2013.

http://avogadro.cc/

^{1}H and ^{13}C spectrum of L1 ligand

---- PROCESSING PARAMETERS ----

dc_balance
saxp : 0.2[Hz]
trapezoid : 0[%] : 0[%] : 80[%] : 100[%]
zerofill : 1
fft : 1
machinephase
ppm

Filename   = K-L1_Proton_ft-1-2.jdf
Author   = datum
Experiment   = proton.jxp
Sample_Id   = K-L1
Solvent   = DMSO-D6
Creation_Time   = 19-SEP-2018 09:44:35
Revision_Time   = 19-SEP-2018 09:31:22
Current_Time   = 19-SEP-2018 09:31:47

Comment   = single_pulse
Data_Format   = 1D COMPLEX
Dim_Size   = 26214
Dim_Title   = Proton
Dim_Units   = [ppm]
Dimensions   = X
Spectrometer   = DELTA2_NMR

Field_Strength   = 9.389766[T] (400[MHz])
X_Acq_Duration   = 3.8535168[s]
X_Domain   = 1H
X_Freq   = 399.78219838[MHz]
X_Offset   = 5[ppm]
X_Points   = 32768
X_Prescans   = 1
X_Resolution   = 0.25950322[Hz]
X_Sweep   = 8.50340136[kHz]
X_Sweep_Clipped   = 6.80272109[kHz]
Irr_Domain   = Proton
Irr_Freq   = 399.78219838[MHz]
Irr_Offset   = 5[ppm]
Tri_Domain   = Proton
Tri_Freq   = 399.78219838[MHz]
Tri_Offset   = 5[ppm]
Clipped   = FALSE
Scans   = 16
Total_Scans   = 16

Relaxation_Delay = 2[s]
Recvr_Gain   = 40
Temp_Get   = 19.9[dC]
X_90_Width   = 11.75[us]
X_Acq_Time   = 3.8535168[s]
X_Angle   = 45[deg]
X_Atn   = 0.5[dB]
X_Pulse   = 5.875[us]
Irr_Mode   = Off
Tri_Mode   = Off

DMSO/Water

7.101
7.119
7.138
7.322
7.342
7.361
7.820
7.839

10.815

2.07
2.06
1.02
1.00

X : parts per Million : Proton

abundance

Filename   = L_1_Carbon-1-3.jdf
Author   = datum
Experiment   = carbon.jxp
Sample_Id   = L_1
Solvent   = DMSO-D6
Creation_Time   = 22-MAY-2019 10:37:13
Revision_Time   = 22-MAY-2019 10:32:44
Current_Time   = 22-MAY-2019 10:33:00
Comment   = single pulse decoupled g
Data_Format   = 1D COMPLEX
Dim_Size   = 26214
Dim_Title   = Carbon13
Dim_Units   = [ppm]
Dimensions   = X
Site   = JNM-ECS400
Spectrometer   = DELTA2_NMR

Field_Strength   = 9.389765[T] (400[MHz])
X_Acq_Duration   = 1.04333312[s]
X_Domain   = 13C
X_Freq   = 100.52530333[MHz]
X_Offset   = 100[ppm]
X_Points   = 32768
X_Prescans   = 4
X_Resolution   = 0.9584665[Hz]
X_Sweep   = 31.40703518[kHz]
X_Sweep_Clipped   = 25.12562814[kHz]
Irr_Domain   = Proton
Irr_Freq   = 399.78219838[MHz]
Irr_Offset   = 5[ppm]
Clipped   = FALSE
Scans   = 336
Total_Scans   = 336

Relaxation_Delay = 2[s]
Recvr_Gain   = 50
Temp_Get   = 20.1[dC]
X_90_Width   = 8.25[us]
X_Acq_Time   = 1.04333312[s]
X_Angle   = 30[deg]
X_Atn   = 4.6[dB]
X_Pulse   = 2.75[us]
Irr_Atn_Dec   = 21.814[dB]
Irr_Atn_Noe   = 21.814[dB]
Irr_Noise   = WALTZ
Irr_Pwidth   = 0.115[ms]
Decoupling   = TRUE

X : parts per Million : Carbon13